Attosecond XUV absorption spectroscopy of doubly excited states in helium atoms dressed by a time-delayed femtosecond infrared laser

Z. Q. Yang,[1,2,3] D. F. Ye,[2,4] Thomas Ding,[4] Thomas Pfeifer,[4] and L. B. Fu[2,*]

[1]*School of Physics, Beijing Institute of Technology, Beijing 100081, China*

[2]*National Key Laboratory of Science and Technology on Computational Physics, Institute of Applied Physics and Computational Mathematics, Beijing 100088, China*

[3]*Key Laboratory of Ecophysics and Department of Physics, College of Science, Shihezi University, Shihezi 832003, China*

[4]*Max-Planck-Institut für Kernphysik, 69117 Heidelberg, Germany*

(Received 10 October 2014; published 27 January 2015)

In the present paper, we investigate the time-resolved transient absorption spectroscopy of doubly excited states of helium atoms by solving the time-dependent two-electron Schrödinger equation numerically based on a one-dimensional model. The helium atoms are subjected to an extreme ultraviolet (XUV) attosecond pulse and a time-delayed infrared (IR) few-cycle laser pulse. A superposition of doubly excited states populated by the XUV pulse is identified, which interferes with the direct ionization pathway leading to Fano resonance profiles in the photoabsorption spectrum. In the presence of an IR laser, however, the Fano line profiles are strongly modified: A shifting, splitting, and broadening of the original absorption lines is observed when the XUV attosecond pulse and infrared few-cycle laser pulse overlap in time, which is in good agreement with recent experimental results. At certain time delays, we observe symmetric Lorentz, inverted Fano profiles, and even negative absorption cross sections indicating that the XUV light can be amplified during the interaction with atoms. We further prove that the above pictures are general for different doubly excited states by suitably varying the frequency of the IR field to coherently couple the corresponding states.

DOI: 10.1103/PhysRevA.91.013414 PACS number(s): 32.80.Qk, 32.80.Zb, 32.80.Fb, 42.50.Gy

I. INTRODUCTION

The rapid development of attosecond technology in the last decade has made it possible to study the time-resolved dynamics of correlated electrons in atoms and molecules [1]. A prominent detection scheme is to shine an attosecond-pulsed extreme ultraviolet (XUV) light together with a synchronized infrared (IR) laser pulse on atoms or molecules, and then measure the photoions, photoelectrons, or the XUV-photoabsorption spectrum. Information on the time-resolved dynamics can be extracted by adjusting the time delay between the XUV and the IR pulses. For instance, this scheme has been successfully applied to measure the duration of an Auger decay [2] and to monitor and control the autoionization dynamics on the attosecond time scale [3,4].

Physically, a single attosecond XUV pump pulse can ionize or excite the atoms via different quantum channels [5]. If the photon energy is high enough, a special kind of doubly excited states can also be populated after the XUV pulse. The energies of such doubly excited states are above the one-electron ionization threshold. Thus they can be viewed as discrete states embedded in the single ionization continuum, and as such are prime examples of autoionizing states. One XUV photon absorption will lead to two different ionization channels: direct ionization and indirect ionization via the autoionization process. These two paths interfere and give rise to the well-known Fano line shape [6].

For the structure and excitation of autoionizing states, electron-electron (*e*-*e*) correlation plays a major role. This fact moved them into the center of scientific interest in recent years [7–9]. Naturally, the helium atom with only two electrons serves as the paradigmatic system for studying this typical *e*-*e* correlation effect. It has been demonstrated that laser-induced ionization and laser-induced coupling between the doubly excited states of the helium atom play an important role in the autoionization process and can modify the Fano resonance profile [10–14]. From the theoretical side, the strong field approximation or few-level models were usually exploited to investigate time-resolved autoionization. However, the former totally ignores Coulomb attraction by the atomic nucleus after ionization and the latter does not fully take into account the complex multilevel coupling. We also note that, albeit great progress has been achieved in solving the full-dimensional Schrödinger equation for laser-dressed two-electron systems (see, e.g., Ref. [15]), a simple one-dimensional model can significantly reduce the computational budget. However, it needs to be verified whether this simplified model can seize the basic physics at work in the attosecond transient absorption experiments. These considerations motivate the current work.

In this paper, by employing a one-dimensional (1D) two-electron (2*e*) model, we investigate the attosecond transient absorption spectroscopy of helium atoms, focusing on the autoionizing resonances. The 1D-2*e* time-dependent Schrödinger equation (TDSE) can be solved numerically with high precision. In our study, the wave packet consisting of doubly excited states is populated by a single broad-bandwidth attosecond XUV pulse. We study the initiated wave-packet oscillations under the influence of a moderately strong few-cycle IR laser pulse with a controlled time delay with respect to the XUV pump pulse, which transiently induces spectral modifications. Our theoretical calculations are compared with recent experiments [13,14].

The paper is structured as follows. Section II is our theoretical model. The main results are presented and discussed in

*lbfu@iapcm.ac.cn

Sec. III. We draw our conclusions in Sec. IV. Atomic units are used throughout the paper unless otherwise specified.

II. THEORETICAL METHOD

For a 1D helium atom, the time evolution of the two-electron wave packet can be obtained by solving the TDSE in the length gauge within the dipole approximation [16],

$$i\frac{\partial\Psi(x_1,x_2,t)}{\partial t}=\left[-\frac{1}{2}\frac{\partial^2}{\partial x_1^2}-\frac{1}{2}\frac{\partial^2}{\partial x_2^2}+V_{ne}(x_1)+V_{ne}(x_2)+V_{ee}(x_1,x_2)+(x_1+x_2)E(t)\right]\Psi(x_1,x_2,t), \tag{1}$$

where x_i $(i=1,2)$ are the coordinates of the two electrons, and $V_{ne}(x_i)=-2/\sqrt{x_i^2+a^2}$ and $V_{ee}(x_1,x_2)=1/\sqrt{(x_1-x_2)^2+b^2}$ are the Coulomb interactions between nucleus and electrons and between the two electrons, respectively. The soft-core parameters are chosen as $a=0.707$ and $b=0.582$ to match the first and second ionization energy of the real helium atom [17]. The external field $E(t)$ is a superposition of an XUV pulse $E_X(t)$ and an IR laser pulse $E_L(t)$. The pulses are linearly polarized in the same direction and defined by

$$E_X(t)=E_{X0}e^{-(2\ln2)(t/\tau_X)^2}\cos\omega_X t \tag{2}$$

and

$$E_L(t)=\begin{cases}0 & \text{if } |t-t_d|\geq 1.375\tau_L\\ E_{L0}\cos^2\left[\frac{\pi(t-t_d)}{2.75\tau_L}\right]\cos[\omega_L(t-t_d)] & \text{otherwise,}\end{cases} \tag{3}$$

respectively. Here, E_{X0} and E_{L0} are the electric-field amplitudes; ω_X and ω_L are the central frequencies of the two pulses; τ_X and τ_L are the pulse durations defined as the full width at half maximum (FWHM) of the laser envelope; and t_d is the time delay between the two pulses, and it is positive if the IR pulse arrives after the XUV pulse.

The TDSE is solved numerically by split-operator methods [18]. The time evolution starts from the singlet ground state which is obtained by imaginary-time propagation from an arbitrary initial state. Absorbing boundaries are employed in order to suppress the unphysical reflection and transmission effects due to the finite size of the system.

We make some remarks before going further. The problem at hand can be handled within a fully *ab initio* framework solving the time-dependent Schrödinger equation in three dimensions [15]. However, the simulation indeed requires a 6 (spatial, even taking symmetry into account, it can only be reduced to 5) +2 (temporal, real time and time delay) dimensional calculation, representing a huge computational task that cannot be handled without the help of large-scale high-performance supercomputers. Thus, it is desirable to test whether a reduced dimensional model can approximate the basic physics and well reproduce the main features observed in the experiments and the full-dimensional *ab initio* calculations. In addition, a 1D model also has many other advantages: (i) it gives one, and others, the opportunity to use such quickly running $1d$ codes to build and test new physics models; (ii) it can be used to check which of the experimentally observed effects may be caused by dimensionality (or angular distributions), and which are just due to fundamental physics; and (iii) it is easier to be extended to even more complex systems such as multielectron systems.

Indeed, such simplified 1D models have been successfully used in the existing literature, e.g., to identify the mechanisms behind nonsequential double ionization [19,20], to study autoionizing resonances in photoelectron spectra [21], and to propose a new molecular imaging method using high-order-harmonic generation and above-threshold ionization [22], to name only a few. Here we extend it to calculate the transient absorption spectrum. In our situation, the weak XUV pulse induces a time-dependent dipole moment in the atom dressed by the IR field, which in turn results in a dipole emission that coherently contributes to the XUV field. For a dilute gas, the relative change of the spectral intensity of the XUV pulse can be expressed in terms of an effective transient absorption atomic cross section $\sigma(\omega)$ [23–25],

$$\sigma(\omega)=-4\pi\alpha\omega\,\mathrm{Im}\left[\frac{\tilde{d}(\omega)}{\tilde{E}(\omega)}\right], \tag{4}$$

where $\tilde{d}(\omega)$ and $\tilde{E}(\omega)$ represent the Fourier transform of the time-dependent dipole moment and the XUV field, respectively. α is the fine-structure constant. The dipole spectrum $\tilde{d}(\omega)$ is calculated via $\tilde{d}(\omega)=-\tilde{a}(\omega)/\omega^2$, where $\tilde{a}(\omega)$ denotes the Fourier transform of the time-dependent dipole acceleration $a(t)$,

$$a(t)=\langle\Psi(x_1,x_2,t)|\sum_i\frac{\partial V_{ne}(x_i)}{\partial x_i}+2E(t)|\Psi(x_1,x_2,t)\rangle \quad (i=1,2). \tag{5}$$

III. MAIN RESULTS

A. Energy levels of doubly excited states and absorption spectrum of an XUV pulse

The energy levels of our 1D helium model atom can be obtained by exploiting the autocorrelation function $C(t)=\langle\Psi(x_1,x_2,t_0)|\Psi(x_1,x_2,t)\rangle$ [18,21]. Here $\Psi(x_1,x_2,t_0)$ is an arbitrary initial state, and $\Psi(x_1,x_2,t)$ is the time-dependent wave function propagating freely from the initial state under the Hamiltonian without external field. A Fourier transform of the autocorrelation function yields some discrete peaks in the frequency domain, which correspond to the energies of the eigenstates contained in the initial state. The energy levels of interest are illustrated in Fig. 1(a). The notation $|n_1,n_2\rangle$ indicates the electron configuration that one electron fills in the state $|n_1\rangle$ of He^+ and the other in $|n_2\rangle$. Here, n_i $(i=1,2)=1,2,3,\ldots$ refer to the ground state, first excited state, second excited state of He^+, and so on. We set the ground state energy to be zero, thus the single ionization potential I_P of He is 24.6 eV. The first six doubly excited states $|2,n\rangle$ $(n=2,3,4,5,6,7)$ are at 45.49, 50.72, 51.47, 52.43, 52.72, and 53.13 eV, respectively. All of them lie above the one-electron ionization threshold.

The absorption spectrum after irradiation with a weak attosecond XUV pulse with FWHM $\tau_X=170$ attoseconds,

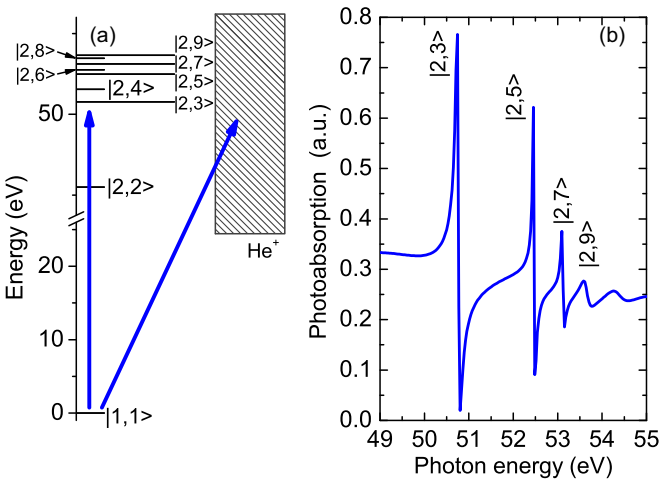

FIG. 1. (Color online) (a) Energy-level diagram of the $|2,n\rangle$ doubly excited states of the 1D helium model atom and (b) absorption spectrum after the irradiation with a single attosecond XUV pulse.

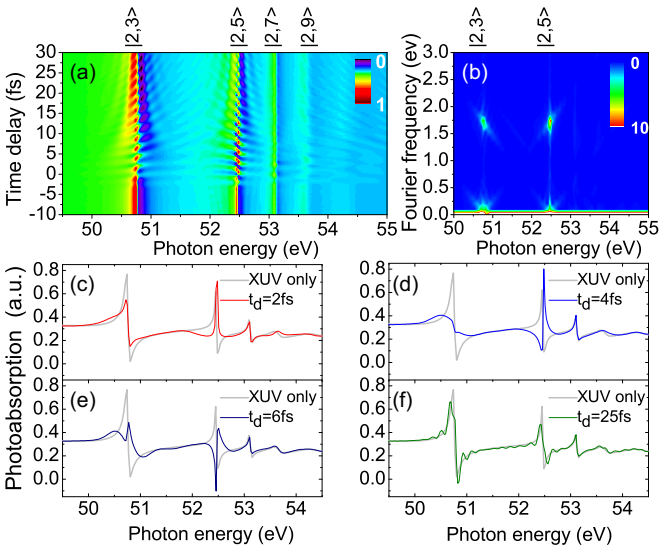

FIG. 2. (Color online) (a) Attosecond transient absorption spectroscopy of XUV in helium as a function of photon energy and time delay between the XUV pulse and the IR laser. (b) Two-dimensional spectrogram obtained from the data shown in (a) by Fourier transformation along the time-delay axis. (c)–(f) Absorption spectra at different time delays.

central photon energy $\omega_X = 1.84$ a.u. $= 50$ eV, and peak intensity 10^{10} W/cm^2 is shown in Fig. 1(b). For the one-photon absorption process, because the ground state is an even-parity state, the atom can only be excited to odd-parity states by the attosecond XUV pulse. In our simulation, the central energy of the XUV pulse is chosen to be close to the energy gap between state $|2,3\rangle$ and the ground state. Therefore only the doubly excited state $|2,3\rangle$ and other odd-parity states around it can be significantly occupied by absorbing one XUV photon. The even-parity states $|2,2\rangle$, $|2,4\rangle$, and $|2,6\rangle$ are not occupied after the XUV pulse. The absorption spectrum exhibits the typical asymmetric absorption lines named as Fano profile [6] induced by the interference of two paths: either direct ionization into the background continuum or indirect ionization from the doubly excited states via the autoionizing resonance. They correspond to the autoionizing states $|2,3\rangle$, $|2,5\rangle$, $|2,7\rangle$, $|2,9\rangle$, and so on, as indicated by the labels in Fig. 1(b).

B. Attosecond transient absorption spectroscopy in the presence of an IR laser pulse with controlled time delay

In this section, we investigate attosecond transient absorption spectroscopy of doubly excited states in the presence of an IR laser pulse. The problem has been experimentally investigated recently [13,14], and further explained by solving the full-dimensional Schrödinger equation [15]. Here, we first perform a comparative study to see whether our calculations based on a simplified one-dimensional model can well reproduce the main structures of the full-dimensional *ab initio* calculations as well as the experimental observations. This is important and must be done before the model can be convincingly used in further calculations and predictions, as discussed in Sec. III C below.

The XUV pulse is the same as in Fig. 1 to excite doubly excited states from the ground state by a one-photon transition. The IR laser peak intensity is 2×10^{11} W/cm^2 in the calculation. Central photon energy ω_L is 0.032 a.u. $= 0.87$ eV, which just matches half of the energy difference between state $|2,3\rangle$ and state $|2,5\rangle$ and can induce a two-photon Rabi oscillation between them. The FWHM duration τ_L of the IR pulse is 6 fs. The photoabsorption spectra of XUV light in helium versus time delay between the XUV pulse and the IR laser are shown in Fig. 2. The overall shape of the photoabsorption spectrum agrees very well with the experimental measurements [13]. As can be seen in Fig. 2(a), for the case that the IR pulse arrives before the XUV pulse, i.e., at large negative time delays, the photoabsorption spectrum displays the characteristic Fano profiles [6] as if there is only an XUV pulse. By contrast, the XUV-absorption spectrum is strongly modified in the presence of the IR pulse near temporal overlap with the XUV pulse: A shifting, splitting, and broadening of the main absorption lines can be clearly observed when the IR and XUV pulses overlap in time [10,26]. By tracing back the time evolution of the population transfer among the ground state and the doubly excited states, we confirm that this is induced by the strong coupling of the doubly excited states and multiple Rabi cycling between the state $|2,3\rangle$ and state $|2,5\rangle$. For the case of large positive time delays, the spectrum converges again to the Fano profiles as obtained for the XUV-only case. However, due to the sharp change in the phase or population of the excited state of the resonances induced by the strong IR pulse, the fringes around the main absorption lines will be observed.

The current photon energy of the dressing IR field, 0.87 eV, is two-photon resonantly coupled to the doubly excited state $|2,3\rangle$ and state $|2,5\rangle$. The spectral structures as well as temporal oscillations throughout the spectrum show that the two lowest doubly excited states $|2,3\rangle$ and $|2,5\rangle$ are most strongly modulated as a function of time delay. The transversal wavelike features visible around both absorption lines of state $|2,3\rangle$ and state $|2,5\rangle$ for positive time delays are slices of the hyperbolic branches $t_d^{(n)}(E) = 2\pi n/|E - E_r|$ (E is the photon energy and E_r is the resonance energy corresponding to the doubly excited state), which is the same as observed in [10,15].

They are caused by the interference of two pathways: direct excitation by absorption of one XUV photon and indirect excitation first to a higher or lower doubly excited state followed by a two-IR-photon transition back to the same state.

In Fig. 2(b), a two-dimensional Fourier-transformed spectrogram is obtained from Fig. 2(a) along the time-delay axis. A similar modulation frequency 1.7 eV is observed in both the $|2,3\rangle$ state and $|2,5\rangle$ state, which is equal to the energy gap between state $|2,3\rangle$ and state $|2,5\rangle$. This proves the coherent coupling of these low-lying doubly excited states by the IR field. That is similar to the experimental results 3.5 eV in both the $|2s2p\rangle$ state and $|sp_{2,3+}\rangle$ state [13]. The diagonal lines originating at each peak (both at 1.7 and 0 eV) are due to off-resonant interference of the natural and laser-dressed two electron dipole responses and further confirm the coherent coupling of these states.

Typical photoabsorption spectra are demonstrated in Figs. 2(c)–2(f) with $t_d = 2$, 4, 6, and 25 fs, respectively. It is interesting to note that, when $t_d = 2$ fs, the Fano profile at the $|2,3\rangle$ state is slightly modified with a different q parameter. For the $|2,5\rangle$ state the asymmetric Fano profile is changed into a symmetric Lorentz profile [see Fig. 2(c)]. At time delay $t_d = 4$ fs, the main Fano profile at the $|2,5\rangle$ state is inverted, while the Fano profile at the $|2,3\rangle$ state is almost depleted [see Fig. 2(d)]. The change of line profile is due to the Rabi cycling between the state $|2,3\rangle$ and state $|2,5\rangle$ induced by the IR pulse [10]. When $t_d = 6$ fs, the Fano profile at the $|2,3\rangle$ state vanishes and two peaks are observed; the absorption cross section in the $|2,5\rangle$ state exhibits a negative value [see Fig. 2(e)], which indicates that the XUV field at that frequency is actually amplified rather than absorbed. This finding has been confirmed by a recent experiment [14]. At a larger time delay of 25 fs [see Fig. 2(f)], the XUV and IR pulses do not overlap in time anymore. For such a delay, the Fano profile is slightly changed as compared with the XUV-only case. The spectrum is accompanied by side peaks which give rise to the hyperbolic interference structures in Fig. 2(a).

C. IR laser frequency modulation

After checking the validity of the 1D model, we use it here to predict the generality of the time-dependent coupling of different autoionizing states by varying the IR frequency.

The attosecond transient absorption spectra shown in Fig. 2 contain rich details of how the dressing laser controls the transition between different states and the absorption of the XUV light. It is observed that only the spectral line shapes of state $|2,3\rangle$ and state $|2,5\rangle$ are strongly modified by the IR pulse in Fig. 2. By contrast, the line shapes of state $|2,7\rangle$ and even higher doubly excited states are apparently not modified. In the following, we show that by changing the frequency of the IR field we are also able to modify the absorption line shapes of higher doubly excited states, and even additional structures are observed in the two-dimensional spectrogram.

For the results shown in Fig. 3, the XUV pulse remains fixed as in Fig. 1, while the IR laser frequency is chosen at 0.046 a.u. = 1.25 eV or 0.054 a.u. = 1.47 eV to resonantly couple higher doubly excited states. The overall features, i.e., the shifting, splitting, and broadening of the main absorption lines are similar to that observed in Fig. 2(a). However, there

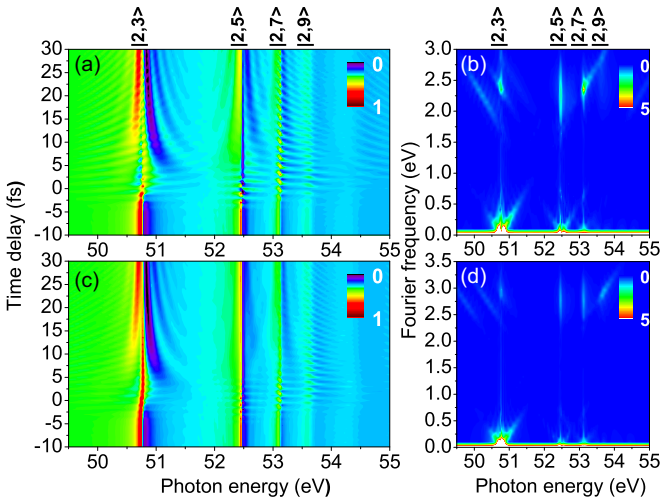

FIG. 3. (Color online) (a) Attosecond transient absorption spectroscopy of XUV light in helium as a function of photon energy and time delay between the XUV pulse and the IR laser. The XUV pulse is the same as in Fig. 1. Peak intensity of the IR pulse is 10^{12} W/cm^2, with pulse duration 6 fs, and central frequency (a) 0.046 a.u. = 1.25 eV, and (c) 0.054 a.u. = 1.47 eV, respectively. (b) and (d) are two-dimensional spectrograms obtained from the data shown in (a) and (c) by Fourier transformation along the time-delay axes.

are some different fine structures. In Fig. 3(a), the spectral structures throughout the spectrum show that the two doubly excited states $|2,3\rangle$ and $|2,7\rangle$ are most strongly modulated as a function of the time delay. Temporal oscillations with a period of $T = 2\pi/(E_{|2,7\rangle} - E_{|2,3\rangle}) = 1.73$ fs confirms the coherent excitation and coupling between these two states. This is because the central frequency of the dressing IR field is 0.046 a.u. = 1.25 eV, which resonantly couples the state $|2,3\rangle$ and state $|2,7\rangle$ via a two-photon transition. Similarly, in Fig. 3(c), the central frequency of the dressing IR field is 0.054 a.u. = 1.47 eV, which resonantly couples the $|2,3\rangle$ and $|2,9\rangle$ states.

In Figs. 3(b) and 3(d), two-dimensional spectrograms are obtained from the data shown in (a) and (c) by Fourier transformation along the time-delay axes. The modulation frequencies are found to be 2.38 and 2.88 eV, in Figs. 3(b) and 3(d), respectively, which are equal to the energy gap between the states $|2,3\rangle$ and $|2,7\rangle$, and states $|2,3\rangle$ and $|2,9\rangle$, respectively. This proves the coherent coupling of different doubly excited states by varying the frequency of the IR field.

IV. CONCLUSION

In this paper, we investigate transient absorption spectroscopy of helium atoms subjected to an XUV and a delayed IR pulse by numerically solving the two-electron 1D TDSE. We find that the Fano line profile is strongly influenced by the delayed IR laser field. Model calculations of resonance shape and resonance peak height versus time delay agree qualitatively with the recent experimental observations, which indicate that a 1D model is an effective scheme to describe some of the essential physical mechanisms at work in these attosecond transient absorption measurements. We have

changed the IR laser frequency to couple different doubly excited states, which causes different interference frequencies throughout the spectrum in the corresponding absorption lines. The line shapes of the photoabsorption spectrum are modulated as a function of time delay, periodically switching between Lorentz and Fano profiles. This means that control of the quantum path interference is possible by suitable timing of an IR pulse with a certain frequency, and the dynamics of the system is captured more comprehensively by time-domain measurements.

ACKNOWLEDGMENTS

We are grateful to Professor J. Liu and Dr. J. Zhao for stimulating discussions. This work is supported by the 973 program (Projects No. 2013CBA01502 and No. 2013CB834100), the NSFC (Grants No. 11274051, No. 11374040, No. 11304018, and No. 11164025), and the European Research Council (ERC-2013-CoG#616783). D.F.Y. also acknowledges the support by the Foundation of President of the China Academy of Engineering Physics (Grant No. 2014-1-029).

[1] F. Krausz and M. Y. Ivanov, Rev. Mod. Phys. **81**, 163 (2009).

[2] M. Drescher, M. Hentschel, R. Kienberger, M. Uiberacker, V. Yakovlev, A. Scrinzi, T. Westerwalbesloh, U. Kleineberg, U. Heinzmann, and F. Krausz, Nature (London) **419**, 803 (2002).

[3] H. Wang, M. Chini, S. Chen, C. H. Zhang, Y. Cheng, F. He, Y. Wu, U. Thumm, and Z. Chang, Phys. Rev. Lett. **105**, 143002 (2010).

[4] S. Gilbertson, M. Chini, X. Feng, S. Khan, Y. Wu, and Z. Chang, Phys. Rev. Lett. **105**, 263003 (2010).

[5] J. Mauritsson *et al.*, Phys. Rev. Lett. **105**, 053001 (2010).

[6] U. Fano, Phys. Rev. **124**, 1866 (1961).

[7] M. Wickenhauser, J. Burgdörfer, F. Krausz, and M. Drescher, Phys. Rev. Lett. **94**, 023002 (2005).

[8] Z. X. Zhao and C. D. Lin, Phys. Rev. A **71**, 060702 (2005).

[9] H. Geiseler, H. Rottke, N. Zhavoronkov, and W. Sandner, Phys. Rev. Lett. **108**, 123601 (2012).

[10] W. C. Chu and C. D. Lin, Phys. Rev. A **85**, 013409 (2012).

[11] Z. H. Loh, C. H. Greene, and S. H. Leone, Chem. Phys. **350**, 7 (2008).

[12] W. C. Chu, S. F. Zhao, and C. D. Lin, Phys. Rev. A **84**, 033426 (2011).

[13] C. Ott, A. Kaldun, L. Argenti, P. Raith, K. Meyer, M. Laux, Y. Zhang, A. Blättermann, S. Hagstotz, T. Ding, R. Heck, J. Madroñero, F. Martín, and T. Pfeifer, Nature **516**, 374 (2014); C. Ott, A. Kaldun, P. Raith, K. Meyer, M. Laux, Y. Zhang, S. Hagstotz, T. Ding, R. Heck, and T. Pfeifer, arXiv:1205.0519.

[14] C. Ott, A. Kaldun, P. Raith, K. Meyer, M. Laux, J. Evers, C. H. Keitel, C. H. Greene, and T. Pfeifer, Science **340**, 716 (2013).

[15] L. Argenti, C. Ott, T. Pfeifer, and F. Martín, arXiv:1211.2566.

[16] R. Grobe and J. H. Eberly, Phys. Rev. Lett. **68**, 2905 (1992).

[17] P. C. Li, X. X. Zhou, G. L. Wang, and Z. X. Zhao, Phys. Rev. A **80**, 053825 (2009).

[18] M. Feit, J. Fleck, and A. Steiger, J. Comput. Phys. **47**, 412 (1982).

[19] M. Lein, E. K. U. Gross, and V. Engel, Phys. Rev. Lett. **85**, 4707 (2000).

[20] Qing Liao, Yueming Zhou, Cheng Huang, and Peixiang Lu, New J. Phys. **14**, 013001 (2012).

[21] J. Zhao and M. Lein, New J. Phys. **14**, 065003 (2012).

[22] Elmar V. van der Zwan and Manfred Lein, Phys. Rev. Lett. **108**, 043004 (2012).

[23] M. B. Gaarde, C. Buth, J. L. Tate, and K. J. Schafer, Phys. Rev. A **83**, 013419 (2011).

[24] R. Santra, V. S. Yakovlev, T. Pfeifer, and Z.-H. Loh, Phys. Rev. A **83**, 033405 (2011).

[25] In contrast to Ref. [23], we have adopted the commonly used Fourier transformation convention, i.e., $\tilde{\varepsilon}(\omega) = \frac{1}{\sqrt{2\pi}} \int_{-\infty}^{\infty} \varepsilon(t) e^{-i\omega t} dt$ and $\varepsilon(t) = \frac{1}{\sqrt{2\pi}} \int_{-\infty}^{\infty} \tilde{\varepsilon}(\omega) e^{i\omega t} d\omega$. Therefore, our Eq. (4) has an overall minus sign.

[26] H. Bachau, P. Lambropoulos, and R. Shakeshaft, Phys. Rev. A **34**, 4785 (1986).